ACS OMEGA

http://pubs.acs.org/journal/acsodf

Article

Designing a Multiepitope Vaccine against Eastern Equine Encephalitis Virus: Immunoinformatics and Computational Approaches

Truc Ly Nguyen and Heebal Kim*

Cite This: *ACS Omega* 2024, 9, 1092−1105

Read Online

ACCESS | Metrics & More | Article Recommendations | Supporting Information

ABSTRACT: Eastern equine encephalitis virus (EEEV) is a significant threat to human and animal populations, causing severe encephalitis, often leading to long-term neurological complications and even mortality. Despite this, no approved antiviral treatments or EEEV human vaccines currently exist. In response, we utilized immunoinformatics and computational approaches to design a multiepitope vaccine candidate for EEEV. By screening the structural polyprotein of EEEV, we predicted both T-cell and linear B-cell epitopes. These epitopes underwent comprehensive evaluations for their antigenicity, toxicity, and allergenicity. From these evaluations, we selected ten epitopes highly suitable for vaccine design, which were connected with adjuvants using a stable linker. The resulting vaccine construct demonstrated exceptional antigenic, nontoxic, nonallergenic, and physicochemical properties. Subsequently, we employed molecular docking and molecular dynamics simulations to reveal a stable interaction pattern between the vaccine candidate and Toll-like receptor 5. Besides, computational immune simulations predicted the vaccine's capability to induce robust immune responses. Our study addresses the urgent need for effective EEEV preventive strategies and offers valuable insights for EEEV vaccine development. As EEEV poses a severe threat with potential spread due to climate change, our research provides a crucial step in enhancing public health defenses against this menacing zoonotic disease.

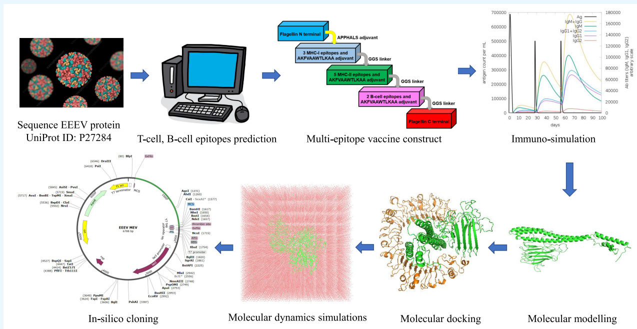

■ INTRODUCTION

Eastern equine encephalitis virus (EEEV) is a member of the genus *Alphavirus* and the family Togaviridae. *Culiseta melanura* mosquitoes, associated with freshwater swamps and marshes, act as the primary vectors for EEEV, where they feed on avian hosts, which serve as the virus's reservoir.[1] The virus undergoes an enzootic cycle, transmitting between birds and mosquitoes.[2] However, other mosquito species, such as *Culex erracticus*, *Anopheles quadrimaculatus*, *Anopheles punctipennis*, *Aedes sollicitans*, *Aedes vexans*, *Coquillettidia perturbans*, and *Culiseta morsitan*, can act as bridge vectors, transmitting the virus between other birds and mammalian hosts, including equines, livestock, and humans.[2,3] EEEV has a predominantly geographically restricted distribution, primarily affecting North America, including the eastern coastal regions of the United States and parts of Canada.[2] However, sporadic cases and outbreaks have also been reported in the Caribbean, Central America, and South America.[2,4,5] The clinical manifestations of EEEV infection can vary widely, ranging from asymptomatic or febrile to severe neurological illness.[6] The incubation period is typically 4 to 10 days.[7] In symptomatic cases, the initial symptoms include fever, muscle ache, nausea, malaise, headache, joint pain, and chills; around five percent of the cases develop meningitis and encephalitis.[6,8] As the disease progresses, individuals may develop neurological symptoms such as seizures, altered mental status, drowsiness, behavioral changes, paralysis, and coma.[6,7] EEEV can cause sepsis and multiple organ failure in patients.[9] Severe cases of EEEV infection have a high fatality rate (41%), with survivors often experiencing long-term neurological complications such as cognitive impairment, paralysis, and seizure.[3,10,11]

EEEV was first isolated and implicated in the etiology of equine disease in 1933 during an outbreak of equine encephalitis in the eastern United States.[1] The confirmation of human infection by the virus occurred in 1938 when the virus was successfully isolated from a human brain during a significant outbreak in Massachusetts, USA.[1,10,12] Since then, EEEV has been recognized as a significant public health concern, because it can cause severe disease in humans and animals. The year 2019 witnessed the most extensive EEEV outbreak in the United States in over half a century. The

Received: September 22, 2023
Revised: November 21, 2023
Accepted: November 27, 2023
Published: December 18, 2023

Table 1. Epitopes Chosen for EEEV Vaccine Candidate[a]

type	epitope	binding affinity	VaxiJen	antigen	allergen	toxicity	IFN	IL4
MHC-I	RAYLIGNKK	124.3	1.1204	Antigen	Nonallergen	Nontoxic	Yes	Yes
	STANIHPAF	226.2	1.5560	Antigen	Nonallergen	Nontoxic	Yes	Yes
	RPTTVNFTV	75.3	1.1955	Antigen	Nonallergen	Nontoxic	Yes	Yes
MHC-II	ISATAWSWL	236.0	1.2212	Antigen	Nonallergen	Nontoxic	Yes	Yes
	ANIHPAFKL	308.9	1.6614	Antigen	Nonallergen	Nontoxic	Yes	Yes
	LIVCMRIVR	535.0	1.2062	Antigen	Nonallergen	Nontoxic	Yes	Yes
	FRPVGREKY	691.7	1.4516	Antigen	Nonallergen	Nontoxic	Yes	Yes
	IIPSTNLEY	1181.3	1.2558	Antigen	Nonallergen	Nontoxic	Yes	Yes
B-cell	PVGREKYRHPPEHGVE	NA	0.9106	Antigen	Nonallergen	Nontoxic	Yes	Yes
	YDFPEYGTGKAGSFGDLQSRTSTSNDLY	NA	0.7421	Antigen	Nonallergen	Nontoxic	Yes	Yes

[a]VaxiJen score above 1.2 for MHC epitopes.

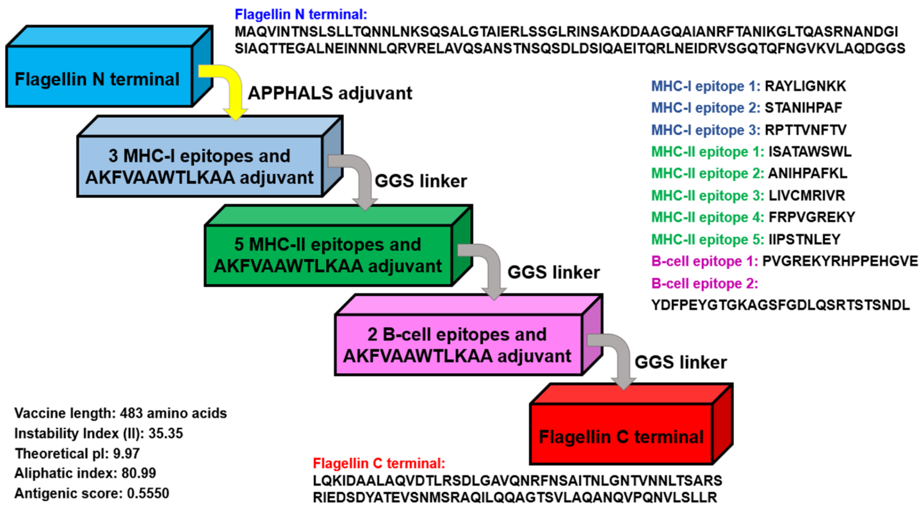

Figure 1. Schematic representation of the vaccine construct with adjuvants, linkers, and epitopes sequentially and appropriately.

outbreak primarily affected the Northeast and Midwest regions of the country, leading to the diagnosis of 38 human cases and 12 deaths.[13,14] Due to its high fatality rate and potential for severe neurological complications, EEEV remains a significant concern for public health. Increased rainfall and rising temperatures due to climate change can cause an increase in the EEEV disease burden and alter the distribution of suitable habitats for the virus, thus raising the possibility of EEEV spreading to new geographic regions.[7]

Currently, no licensed vaccines or specific treatments are available for EEEV infection in humans. However, several ongoing research projects exist to develop and test potential vaccines against EEEV, such as a phase 1/2 clinical trial study of an inactivated EEEV vaccine by Pierson et al.[15] Their findings indicated the vaccine's safety and immunogenicity with improved efficacy after a prolonged primary series. Another study by Coates et al.[16] focused on a trivalent virus-like particle (VLP) vaccine, demonstrating the VLPs' ability to induce neutralizing antibodies against three alphaviruses causing encephalitis. This highlights the need for further development and evaluation in the phase 2 trials. Besides inactivated and VLP vaccines, multiepitope vaccine (MEV) is a promising strategy against viral infections.[17] Via this letter, the author discussed the advantages of developing multiepitope vaccines, composed of a series of or overlapping peptides that can elicit cellular and humoral immune responses against viral infections. The author concluded that well-designed multiepitope vaccines could become powerful prophylactic and therapeutic agents against viral infections. Hence, the primary purpose of our study is to design a multiepitope vaccine candidate for protecting humans from EEEV by employing immunoinformatics and computational vaccinology approaches. The structural polyprotein of the virus was examined using various web servers to predict multiple highly antigenic B-cell and T-cell epitopes. These epitopes were selected based on their nonallergic nature and potential to induce cytokine production, including interleukins and interferon. To design the vaccine, these epitopes were connected by using a GGS linker and supplemented with two adjuvants. Additionally, the Pan HLA DR-binding epitope sequence (PADRE) was included. Computational analyses were conducted to evaluate the antigenic potential, allergenicity, and physicochemical characteristics of the vaccine candidate. Furthermore, the tertiary structure of the vaccine construct was modeled and validated. Molecular docking and molecular dynamics simulations assessed the vaccine's binding ability with Toll-like receptor 5 (TLR5).[18] Finally, computational immune simulation was performed to predict the candidate EEEV vaccine's capability to stimulate an immune response in humans. This study provides valuable insights for EEEV prevention strategies and vaccine development to contribute to the prevention of the potential spread of this zoonotic disease due to climate change.

https://doi.org/10.1021/acsomega.3c07322
ACS Omega 2024, 9, 1092−1105

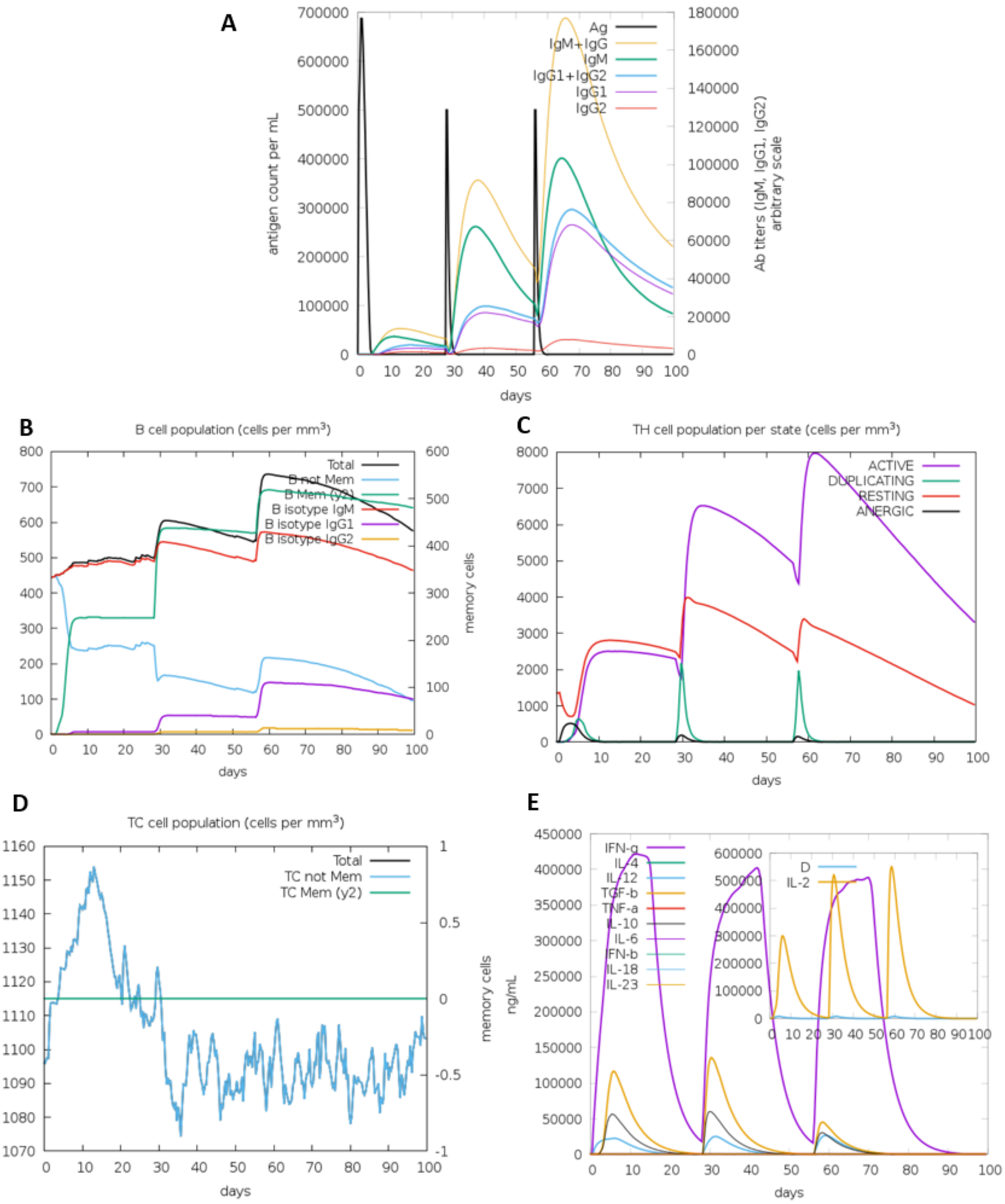

Figure 2. EEEV vaccine immune simulation. (A) Antigen count and antibody titer with a specific subclass. (B) B-cell population. (C) TH-cell population per state. (D) TC-cell population. (E) Cytokines and interleukins.

RESULTS

Epitopes Prediction and Selection of Final Epitopes for the Vaccine Design. The UniProt ID of the EEEV (strain va33) structural glycoprotein is P27284, and the protein has 1240 amino acids. In UniProt, the evidence for the existence of the protein is available at the protein level and has an annotation score of 5/5. A total of 292 MHC class II binding epitopes that strongly bind to the selected HLA alleles were predicted from the EEEV structural polyprotein. These predicted strong binder MHC class II epitopes can be found in Supplementary Data Sheet 1. Similarly, the EEEV structural polyprotein was found to have 126 MHC class I epitopes that strongly bind. The MHC class I epitopes, predicted to be strong binders, are listed in Supplementary Data Sheet 2. Weakly binding peptides to MHC class I or MHC class II were excluded from further analysis. In total, 20 linear B-cell epitopes, with a length between 9 and 30 amino acids, were predicted from both EEEV structural polyproteins (Supplementary Data Sheet 3). The strong binding T-cell epitopes and B-cell epitopes were assessed for toxicity, antigenicity, and allergenicity as well as their ability to activate interferon-γ, interleukin-2, and interleukin-4 production. For detailed

https://doi.org/10.1021/acsomega.3c07322
ACS Omega 2024, 9, 1092−1105

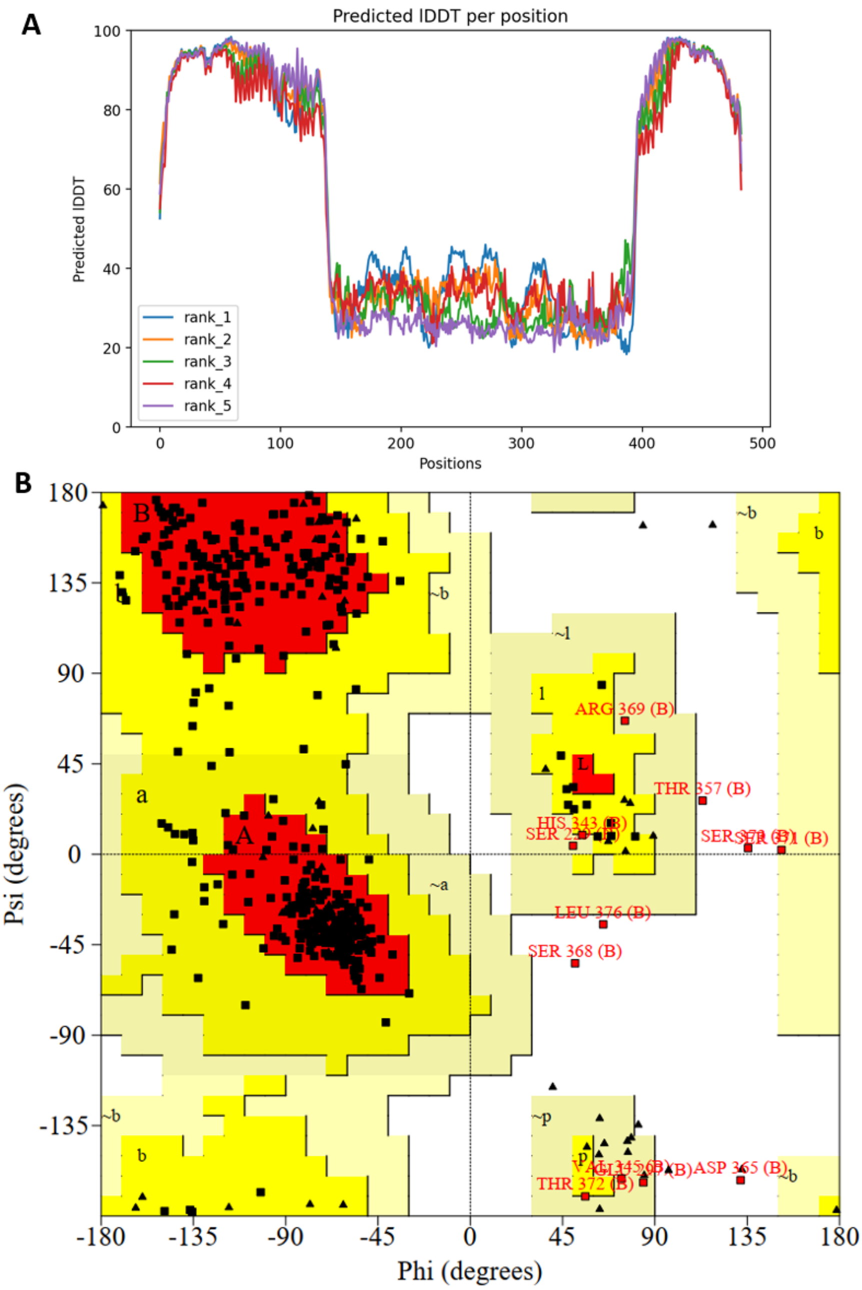

Figure 3. Molecular modeling of EEEV-MEV. (A) Predicted lDDT per position using ColabFold: AlphaFold2. (B) Ramachandran plot using the ProCheck Web server.

information about these T helper, T cytotoxic, and B-cell epitopes attribute, refer to Supplementary Tables S1, S2, and S3. Ultimately, ten strong binding epitopes (2 B-cell, 3 T-cytotoxic, and 5 T-helper) were selected for vaccine design based on their predicted antigenicity, nonallergenicity, and nontoxicity and their ability to stimulate interferon-γ and IL-4 production. These epitopes are listed in Table 1. The selected epitopes for the final vaccine design can potentially cover 60.87% of the world population.

EEEV Vaccine Designing and Prediction of Physicochemical Properties. The chosen ten epitopes were connected to adjuvants by employing a linker to form a stable vaccine construct (instability index = 35.35) for safeguarding against EEEV infection. This construct, which comprises 483 amino acids, exhibits nonallergenic and antigenic properties. The amino acid sequence and the physiochemical characteristics of the vaccine construct are provided in Figure 1.

Immunosimulation of the Designed EEEV Vaccine. Figure 2 illustrates the predicted immune response profile of the designed EEEV-MEV using computational analysis. When the first dose (Figure 2A) was compared to the second and third doses, it was observed that the concentrations of IgM + IgG, IgM, IgG1 + IgG2, IgG1, and IgG2 antibodies increased, which suggests that immunization with the candidate EEEV vaccine leads to an enhanced antibody response. Furthermore, consecutive administrations of the vaccine caused an increase in the total B-cell population and B-memory-cell populations, demonstrating the stimulation of a strong secondary immune response (Figure 2B). Moreover, the vaccination with the designed EEEV vaccine also increased the population of active

https://doi.org/10.1021/acsomega.3c07322
ACS Omega 2024, 9, 1092−1105

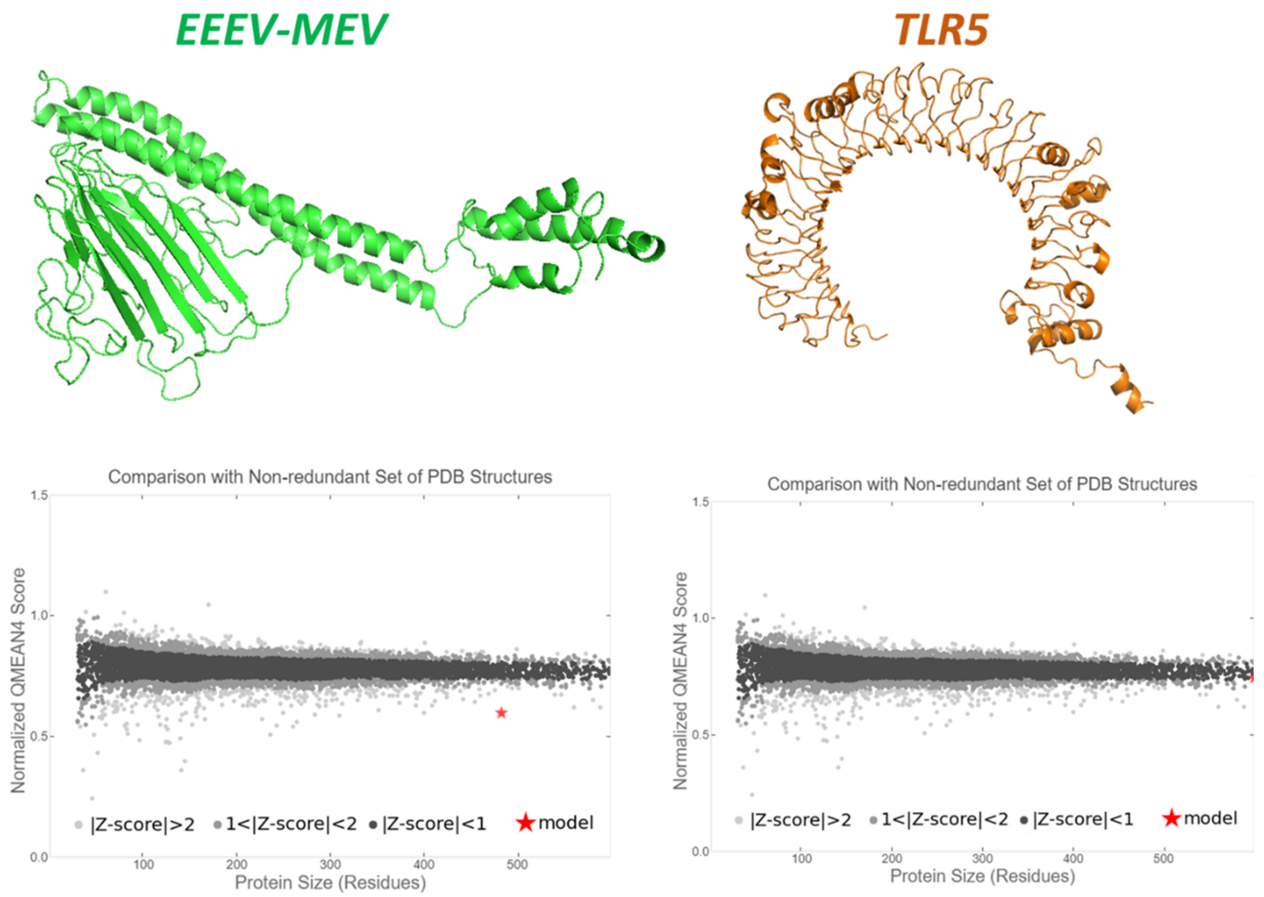

Figure 4. Depiction in cartoon form displaying the 3D models of the EEEV-MEV construct and the TLR5 receptor employed in this investigation. Corresponding quality scores assessed through QMEANS4 are presented below the projected structures.

T-helper cells (Figure 2C). Following the first two injections, the numbers of duplicating and resting T-helper cells showed an increase. However, after the third injection, their population slightly decreased (Figure 2C). The T-cytotoxic memory cell population increased after the first vaccination. Still, after the second and third doses, their population decreased significantly (Figure 2D). Furthermore, the EEEV vaccination exhibited the ability to stimulate various cytokine generations such as IFN-γ, interleukin-10 (IL10), interleukin-12 (IL12), and transforming growth factor-β (TGF-β) (Figure 2E). In comparison to the first dose, the second dose of the vaccine led to increased populations of IL-10, IL-12, and TGF-β but reduced the IFN-γ population. Upon receiving the third dose of the EEEV vaccine, there was an overall decrease in the concentration of different cytokines and interleukins compared to the first and second doses.

Molecular Modeling. The tertiary structures of both the EEEV-MEV construct and the immunogenic TLR5 receptor were predicted through AlphaFold2 via ColabFold. Due to the absence of an experimental structure for TLR5, UniProt ID D1CS82 was obtained from the AlphaFold2 prediction. The yield of high pLDDT values with confidence scores exceeding 90 for most residues indicated a high level of prediction confidence (Figure S1). The focus was particularly directed at amino acids 21−639 in the topological domain, crucial for the interaction with the extracellular signal, while other residues were excluded from the analysis. The structural prediction of the EEEV-MEV vaccine construct using AlphaFold2 yielded pLDDT values above 90 for the N- and C-terminal regions where the flagellin sequence is inserted. However, regions containing adjuvants/linkers and epitope sequences showed low confidence scores with pLDDT values below 50 (amino acids 140−390) (Figure 3A). To validate the predicted structures' quality, Ramachandran plots were calculated for both the modeled TLR5 and the EEEV-MEV vaccine construct. For the EEEV-MEV construct, among the 483 amino acid residues, 83.6% fell within core-favored regions, 15.2%, in allowed and generously allowed regions, and the remaining 1.2%, in disallowed regions (Figure 3B). In the TLR5 receptor, 80.8% of amino acids were within the core-acceptable region and 19.2% were within the allowed and generously allowed regions (Figure S2). Furthermore, the accuracy of the predicted tertiary structures was validated alongside QMEANS4 quality scores (Figure 4).

In addition, the stability of the vaccine construct was assessed via conducting MD simulations using GROMACS software. Initially, a 10 ns equilibration step was performed by using the NPT ensemble. The resulting structure from this equilibration phase was designated as the initial structure, which was utilized for further equilibration and a subsequent 100 ns of production simulation. In Figure 5A, we demonstrate the alignment between the backbone of the vaccine's structure obtained from AlphaFold2 (I) and the 10 ns equilibrated structure (II) of EEEV-MEV. Additionally, Figure 5B illustrates the root-mean-square deviation (RMSD) by comparing the initial equilibrated structure (II) with the coordinate obtained from the 100 ns simulation.

https://doi.org/10.1021/acsomega.3c07322
ACS Omega 2024, 9, 1092−1105

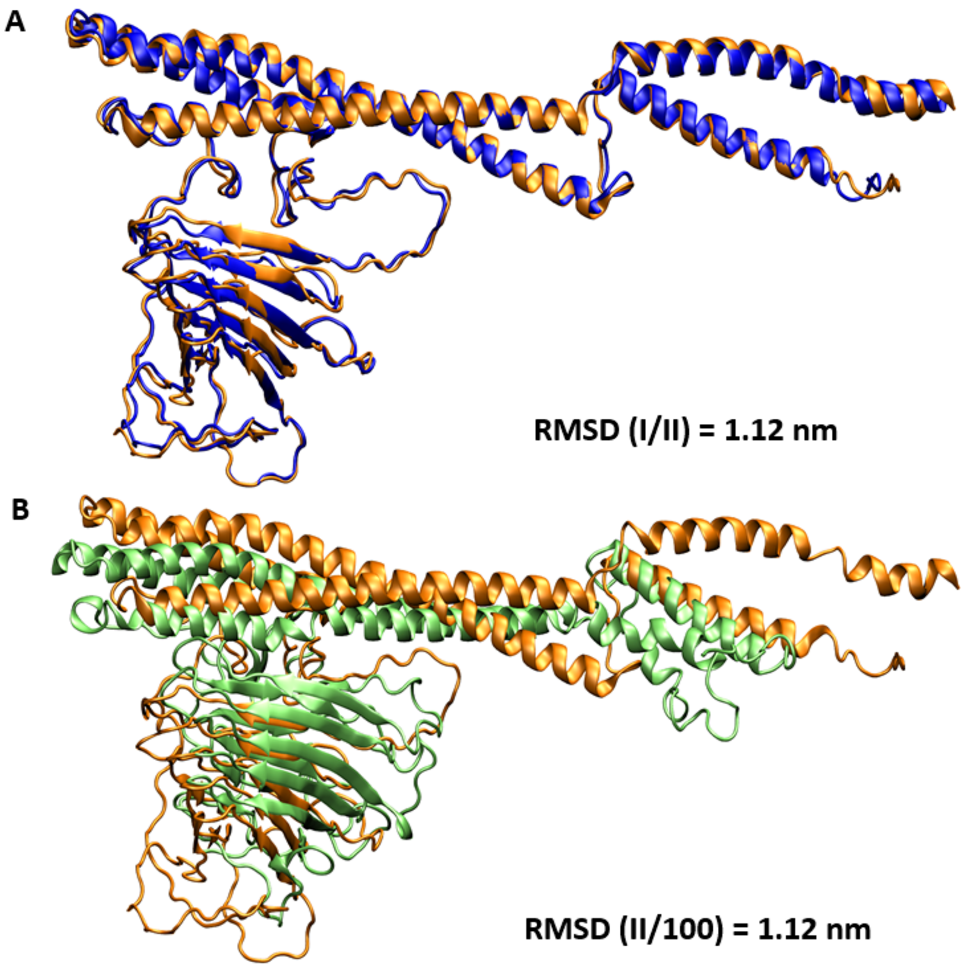

Figure 5. 3D structure of the designed vaccine. (A) Alignment was carried out using the backbone of the EEEV-MEV structure (I) shown in blue and the structure obtained after 10 ns of equilibration (II) shown in orange. (B) Alignment between the initial equilibrated structure after 10 ns (II) and the structure obtained after 100 ns of production simulation.

Molecular Docking. Interaction between the EEEV-MEV construct and TLR5 was assessed via a molecular docking study using the HADDOCK 2.4 Web server with default parameters. The docking approach was information-driven, necessitating the knowledge of specific interacting residues. Based on predictions of Jacchieri et al.,[18] sequences "LQRV-RELAVQ" and "EILDISRNQL" were identified as potential binding sites in flagellin and human TLR5, respectively. Consequently, these sequences were designated as "Active Residues" during the HADDOCK program execution.[19,20] The top-ranked cluster with the lowest HADDOCK score was selected as the final EEEV-MEV and TLR5 complex structure. Finally, the contact maps, specifically distance range maps, were computed for the docked complex using the COCO-MAPS tool.[21] Employing a 5 Å cutoff distance to define contacts, 25 atomic pair contacts were observed between hydrophilic residues, 35, between hydrophilic and hydrophobic residues, and 32, between two hydrophobic residues (Figure 6).

Besides, interacting residues between EEEV-MEV and TLR5 were analyzed using the PDBsum Web server.[22] A total of 8 hydrogen bonds (blue lines), 4 salt bridges (red lines), and 57 nonbonded contacts (orange dashed line) are indicated in Figure 7 and Table 2.

Molecular Dynamics Simulation. To assess the stability of the docked complex between EEEV and TLR5, we conducted MD simulations using GROMACS software, and the results of these simulations are presented in Figure 8. We also conducted additional trial simulations, initiated from a different velocity, in order to validate the robustness of our simulations. The outcomes of these trials are illustrated in Figure S3. Encouragingly, the results from these trial simulations align with those presented in Figure 8. The root-mean-square deviation (RMSD) graph for TLR5 and EEEV is displayed in Figure 8A. The average RMSD values for TLR5 and EEEV were found to be 0.45 ± 0.02 and 0.87 ± 0.10 Å, respectively. The RMSD values reached a stable plateau after 60 ns for EEEV and 40 ns for TLR5. Notably, between 45 and 52 ns, an abrupt increase in RMSD was observed for EEEV, followed by stabilization. This observation suggests that TLR5 remained stable throughout the simulations, while the predicted EEEV vaccine exhibited flexibility due to epitopes and linker regions forming loops. Furthermore, the root-mean-square fluctuation (RMSF) parameter was separately plotted for TLR5 and the vaccine construct to identify highly flexible regions associated with increased fluctuations. As depicted in Figure 8B, the RMSF values for TLR5 and EEEV were determined to be 0.19 ± 0.1 and 0.40 ± 0.2 nm, respectively, indicating higher flexibility in EEEV than TLR5. The average number of hydrogen bonds (H-bonds) between TLR5 and EEEV was quantified and is presented in Figure 8C, with a value of 8 ± 3. Additionally, the interaction energies between

https://doi.org/10.1021/acsomega.3c07322
ACS Omega 2024, 9, 1092−1105

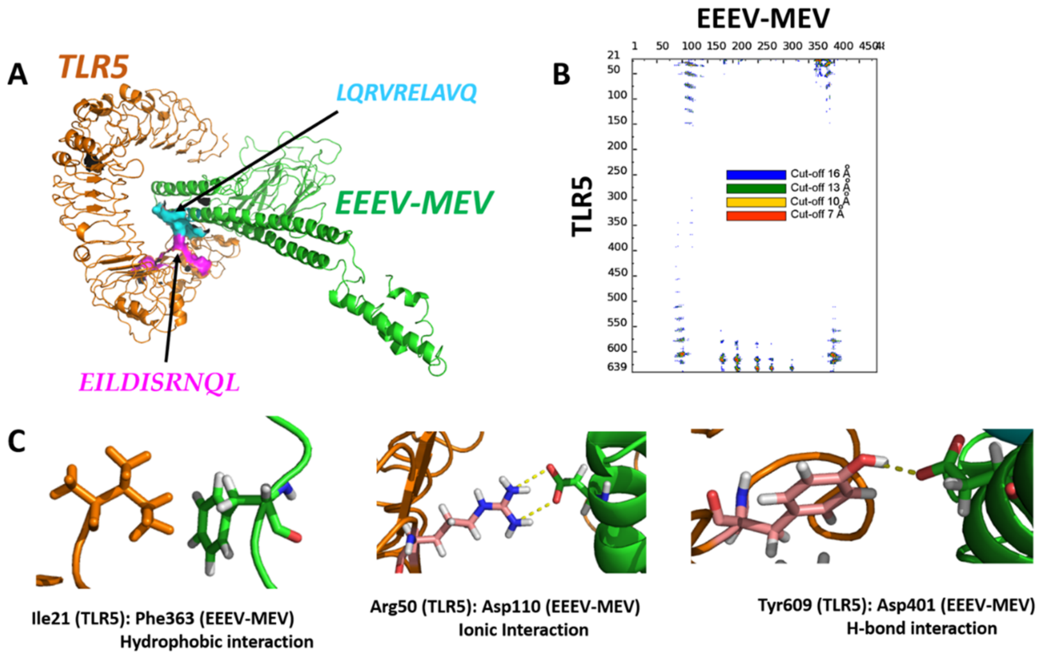

Figure 6. Docked complex depicts the EEEV-MEV construct (green cartoon) and TLR5 (orange cartoon). (A) Surface representations highlight hotspot residues essential for information-driven docking, colored cyan for the EEEV-MEV construct and magenta for TLR5. (B) Distance contact maps illustrate residue interactions between EEEV-MEV and TLR5. (C) Three illustrative interactions involving amino acid residues of the immunogenic receptor TLR5 and the EEEV-MEV construct.

A

Chain	No. of interface residues	Interface area ($Å^2$)	No. of salt bridges	No. of disulphide bonds	No. of hydrogen bonds	No. of non-bonded contacts
A	11	879	4	-	8	57
B	17	869				

B

Figure 7. Interactions between TLR5 (chain A) and EEEV-MEV (chain B) using the PDBsum Web server. (A) Interface statistics. (B) Residue interactions across the interface, hydrogen bonds (blue lines), nonbonded contacts (orange dashed line), and salt bridges (red lines) between residues on either side of the vaccine-TLR5 interface.

TLR5 and the EEEV construct were calculated. The interaction energy was further decomposed into Coulombic interactions, representing the electrostatic interactions and Lennard-Jones (LJ) potential, accounting for the van der Waals interactions. Figure 8D illustrates the interaction energy between TLR5 and EEEV, with the Coulombic and LJ contributions calculated as -148.7 ± 22 and -73.7 ± 11 kcal/mol, respectively. These values indicate that the Coulombic contribution or electrostatic interactions play a dominant role in defining the interaction between TLR5 and EEEV. The buried solvent-accessible surface area (SASA) is presented in Figure 8E, which indicates that the surfaces of TLR5 and EEEV come into direct contact and form various interactions, including hydrogen bonds, electrostatic interactions, and hydrophobic interactions. The graph demonstrates that the interaction remains stable throughout the simulations.

For further assessment of the complex's structural stability, we conducted superimpositions of complex structures extracted from selected snapshots during the simulation. These analyses revealed substantial overlap, yielding RMSD values consistently below 1 nm (Figure 9). Notably, limited flexibility was exclusively observed in the peripheral regions of the EEEV-MEV construct. This observation aligns with recent studies, indicating a similar trend when flagellin was introduced as an adjuvant for vaccine design.[19,20] Within the same selected snapshots, an interface analysis was conducted by utilizing the COCOMAPS tool (Figure 9). In particular, distance range maps were plotted, with dots at the juncture of two residues from the EEEV-MEV construct and TLR5. These dots were color-coded: red, yellow, green, and blue, signifying atom pairs within distances of 7, 10, 13, and 16 Å, respectively. Figure 9 shows that the interface's inter-residue contacts remain consistent and stable for the selected snapshots. This observation holds, despite the observed peripheral flexibility of the EEEV-MEV construct.

Codon Adaptation and Computational Cloning of the Designed EEEV Vaccine. Codon adaptation is necessary to expedite the expression of EEEV-MEV in prokaryotic hosts and facilitate large-scale commercial production. After employing the JCat Web site for codon adaptation in *E. coli*, the Codon Adaptation Index (CAI) value and the guanine−cytosine content (GC content) were found to be 0.9443 and 52.59%, respectively (Supplementary Table S4). For insertion into the pET28a(+) vector, the vaccine construct was

https://doi.org/10.1021/acsomega.3c07322
ACS Omega 2024, 9, 1092−1105

Table 2. List of Atom−Atom Interactions Across the Vaccine-TLR5 Interface

TLR5						EEEV-MEV				
Hydrogen bonds										
No.	Atom no.	Atom name	Res. name	Res. no		Atom no.	Atom name	Res. name	Res. no	Distance
1	474	NH1	ARG	50	⟷	11492	OD1	ASP	110	3.17
2	8622	NH1	ARG	557	⟷	11274	OE1	GLU	94	2.78
3	8625	NH2	ARG	557	⟷	11275	OE2	GLU	94	2.74
4	9390	OD2	ASP	607	⟷	11258	NH2	ARG	93	2.82
5	9425	OH	TYR	609	⟷	15652	OD2	ASP	401	2.73
6	9502	OD1	ASP	614	⟷	12845	NZ	LYS	204	2.76
7	9516	O	SER	615	⟷	12871	N	ALA	207	2.71
8	9554	O	GLY	618	⟷	15597	NE2	GLN	398	2.88
Salt bridges										
1	477	NH2	ARG	50	⟷	11493	OD2	ASP	110	2.99
2	8625	NH2	ARG	557	⟷	11275	OE2	GLU	94	2.74
3	9390	OD2	ASP	607	⟷	11258	NH2	ARG	93	2.82
4	9502	OD1	ASP	614	⟷	12845	NZ	LYS	204	2.76

positioned between the XhoI (158) and *Eco*RI (192) restriction sites. Figure 10 illustrates the final cloned vaccine construct, while the inserted vaccine construct is highlighted in green.

■ DISCUSSION

EEEV is a mosquito-borne pathogen that has garnered increasing attention due to its detrimental impact on human and animal populations. As a member of the genus *Alphavirus* and the family Togaviridae, EEEV is known for its ability to cause severe encephalitis and meningitis, leading to high mortality rates and long-term neurological complications in survivors.[3,10] With a complex transmission cycle involving avian reservoir hosts, mosquito vectors, and mammalian amplifying hosts, the virus poses significant challenges to disease control and prevention efforts. EEEV has been detected in various organisms, including 35 mosquito species, over 200 bird species, multiple livestock, reptiles, amphibians, and wild mammals.[2] Despite its classification as a rare disease, EEEV outbreaks have been recorded across several regions, including the eastern coastal areas of North America, the Caribbean, and some Central and South American nations.[2,4,5] Furthermore, there are no effective antiviral treatments or approved human vaccines for protection against EEEV. Moreover, the continuous increase in reported cases over a broader geographic area, as observed by the upward trend in annual case totals in the United States since 2003, clearly indicates that EEEV is a significant emerging pathogen.[6,7]

EEEV is an enveloped, positive-sense, single-stranded RNA virus.[23] Its genome is approximately 11.7 kilobases in length and contains two open reading frames (ORFs).[3,24] The first ORF encodes the nonstructural proteins, nsP1 to nsP4, responsible for viral replication and processing of polyprotein. In contrast, the second ORF encodes the five structural proteins, including the capsid, envelope glycoprotein 1 (E1), envelope glycoprotein 2 (E2), envelope glycoprotein 3 (E3), and 6K/TF.[3,10,24] The structural proteins involve membrane fusion, virus attachment and penetration, host cell recognition, virion assembly, and maturation.[25,26] The nonstructural proteins of EEEV are not packaged in the final virions, which means that the humoral immune response primarily focuses on the prominent structural proteins found on the surface of the virions.[10] These surface proteins are the main targets of various vaccine and antiviral approaches to combating EEEV.[10] Dupuy et al. used the EEEV structural proteins (E3-E2-6K-E1) to develop a DNA vaccine against EEEV.[27] Another study targeted the EEEV structural protein for developing a recombinant modified vaccinia virus-based vaccine.[28] Hence, in this study, the structural proteins of the EEEV were used to design a multiepitope vaccine candidate for protection from EEEV in humans using immunoinformatics methods. The current work is the first study where the immunoinformatics approach has been employed for vaccine candidate development against EEEV. Vaccine for administration in equines for protection against EEEV is available commercially; however, EEEV vaccines for human use have not been approved yet.[10] Previously, various studies have been conducted to develop vaccine candidates against EEEV. Various options have been investigated as potential vaccine approaches, such as live attenuated vaccines, chimeric virus vaccines, subunit vaccines, virus-like particles (VLPs), and nucleic acid vaccines.[27−31] A study conducted by Ko et al. in 2019 demonstrated that a vaccine candidate for EEEV based on VLPs was highly effective in generating a strong immune response in mice.[31] Subsequently, the vaccine was evaluated in cynomolgus macaques by administering two doses of VLPs intramuscularly. The vaccinated animals produced neutralizing antibodies and were exposed to wild-type viruses through an aerosol route. All vaccinated animals remained infection-free and exhibited no signs of brain tissue damage. At the same time, most of the control group showed signs of viral encephalitis and died within a week.[31] Recently, in a Phase-1 clinical trial, a trivalent VLP-based vaccine against EEEV, western equine encephalitis virus, and Venezuelan equine

https://doi.org/10.1021/acsomega.3c07322
ACS Omega 2024, 9, 1092−1105

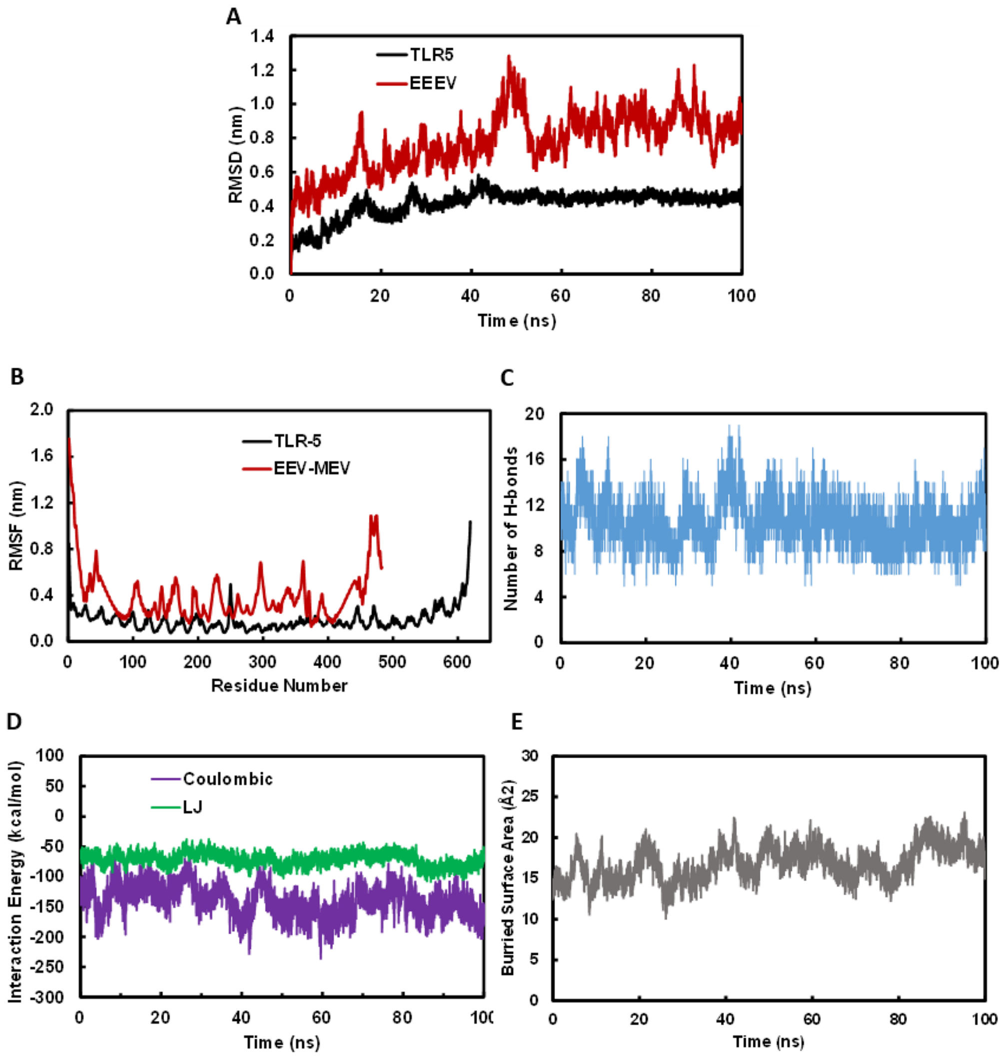

Figure 8. MD simulation of the designed vaccine and the immunogenic receptor TLR5. (A) Time evolution of the Cα RMSD for the TLR5 and EEEV vaccine during MD simulations. (B) Cα RMSF plots depicting the flexibility of the TLR5 and EEEV vaccine. (C) Time evolution of the number of hydrogen bonds between TLR5 and EEEV-MEV during the MD simulations. (D) Variation in interaction energies between the TLR5 and EEEV vaccine, with the electrostatic (Coulombic) and van der Waals (LJ) components segregated. (E) Buried surface area of the TLR5 and EEEV vaccine, indicating the contact area between the two proteins.

encephalitis virus was reported to be safe and well-tolerated and induced neutralizing antibodies.[32]

In this study, multiple T-cell and linear B-cell epitopes were predicted from the structural polyprotein of EEEV. These predicted epitopes underwent further analysis to assess their antigenicity, ability to stimulate cytokine production, toxicity, and allergenicity. Among them, 10 epitopes (3 T-cytotoxic, 5 T-helper, and 2 linear B-cell epitopes) were identified as suitable candidates for the design of an EEEV vaccine. These selected epitopes have the potential to provide coverage for 60.87% of the global population. To create the final vaccine design, the selected epitopes were linked with adjuvants using a linker, resulting in a vaccine construct that is nonallergenic, antigenic, and stable for protection against EEE disease. Molecular docking and molecular dynamics simulations revealed a stable interaction pattern between the vaccine candidate complex and TLR5 receptor. Furthermore, computational immune simulation predicted that the vaccine candidate has the capacity to induce robust immune responses in vaccinated individuals.

■ CONCLUSIONS

This study addresses the immediate need for effective preventive strategies against EEEV, a mosquito-borne pathogen associated with severe encephalitis in humans and animals. The absence of approved antiviral treatments or human vaccines for EEEV underscores the urgency of our research. This work utilized innovative immunoinformatics and computational approaches that comprehensively designed and evaluated a multiepitope vaccine candidate against EEEV. Developing this vaccine construct with exceptional antigenic properties, devoid of toxicity and allergenicity, strong immune responses, and stability, signifies a crucial step toward combating EEEV. Our study provided valuable insights for EEEV vaccine development to contribute to prevention of the potential spread of this zoonotic disease due to climate change. However, further experimental validation and preclinical studies are necessary to ensure vaccine immunogenicity and protective efficacy.

https://doi.org/10.1021/acsomega.3c07322
ACS Omega 2024, 9, 1092−1105

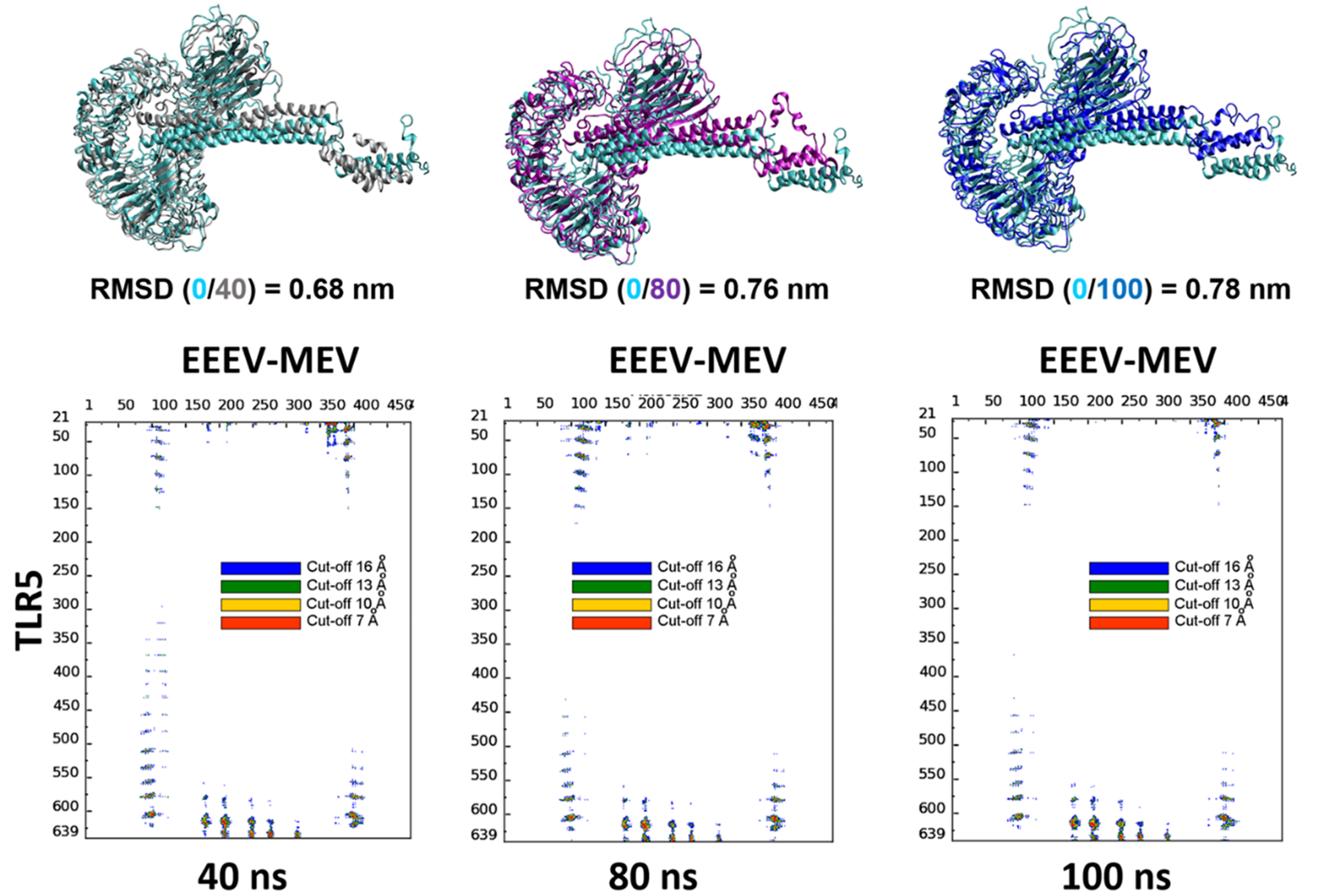

Figure 9. Comparative visualization of chosen snapshots for TLR5 and EEEV-MEV constructs, accompanied by their respective RMSD values. Contact maps highlight the intermolecular interactions for these snapshots. Dots at the intersection of two residues are color-coded (red, yellow, green, and blue), indicating the proximity of atom pairs within 7, 10, 13, and 16 Å distances.

MATERIALS AND METHODS

Retrieval of Amino Acid Sequence, Epitope Prediction, and Selection of Final Epitopes. The amino acid sequence of the EEEV structural polyprotein was obtained from the UniProt database with the ID P27284.[33] The NETMHC 2.3 Web site was utilized to predict T-helper cell epitopes that could potentially bind to MHC class II molecules.[34] In addition, the NetMHCpan 4.0 Web site was used to predict T-cytotoxic cell epitopes that may bind to MHC class I molecules.[35] The protein sequences were entered in FASTA format as inputs, with a selected peptide length of 9, on the NETMHC 4.0 and NETMHC 2.3 Web servers. The chosen HLA alleles for predicting T-helper cell epitopes and T-cytotoxic cell epitopes are listed in Supplementary Data Sheets 1 and 2, respectively. The default parameters of the NETMHC 4.0 and NETMHC 2.3 Web servers were utilized to set the thresholds for strong and weak binders. To predict multiple linear B-cell epitopes, the IEDB B-cell epitope prediction Web site, which operates the Bepipred linear epitope prediction approach, was employed.[36] The VaxiJen version 2.0 Web server was used to determine the antigenicity of the predicted B-cell and T-cell epitopes.[37] To assess the epitope's allergic potential, toxicity, and interferon-γ activation potential, the allergenFP, ToxinPred, and IFNepitope Web servers were used, respectively.[38−40] The ability of the epitopes to induce interleukin-4 generation was assessed using the IL4Pred server.[41]

Population Coverage Analysis of Selected Epitopes. The population coverage analysis tool, available on the Immune Epitope Database and Analysis resource Web site, assessed the population coverage of the chosen epitopes for designing the EEEV vaccine.[42] Nevertheless, there was a limitation in determining the population coverage of the selected B-cell epitopes, as there was a lack of available web servers or software capable of predicting it. Default settings of the server were used except for the "select area(s) and population(s)" option, which was set as "World" and "select calculation option", where the "Class I and II combined" option was selected.

Design and Prediction of Physicochemical Properties of the EEEV-MEV. The selection of B-cell and T-cell epitopes for the final vaccine design was based on their predicted ability to induce interleukin-4 and IFN-γ production and their nontoxicity, nonallergenicity, and antigenicity. Adjuvants, including PADRE, RS09, and *Salmonella dublin* flagellin protein sequences, were incorporated into the vaccine design as in previous studies.[43−45] These adjuvants were connected to the chosen epitopes through "GGS" linkers. It is important to note that a similar approach has been previously employed for vaccine design targeting other viral and fungal pathogens, such as monkeypox virus, *Candida dubliniensis*, and *Candida tropicalis*.[46−48] To assess the allergenic potential, physiochemical properties such as instability index (II), isoelectric point theoretical pI, etc. were evaluated using AllergenFP and ExPASyProtParam tools. The antigenicity of the final vaccine

https://doi.org/10.1021/acsomega.3c07322
ACS Omega 2024, 9, 1092−1105

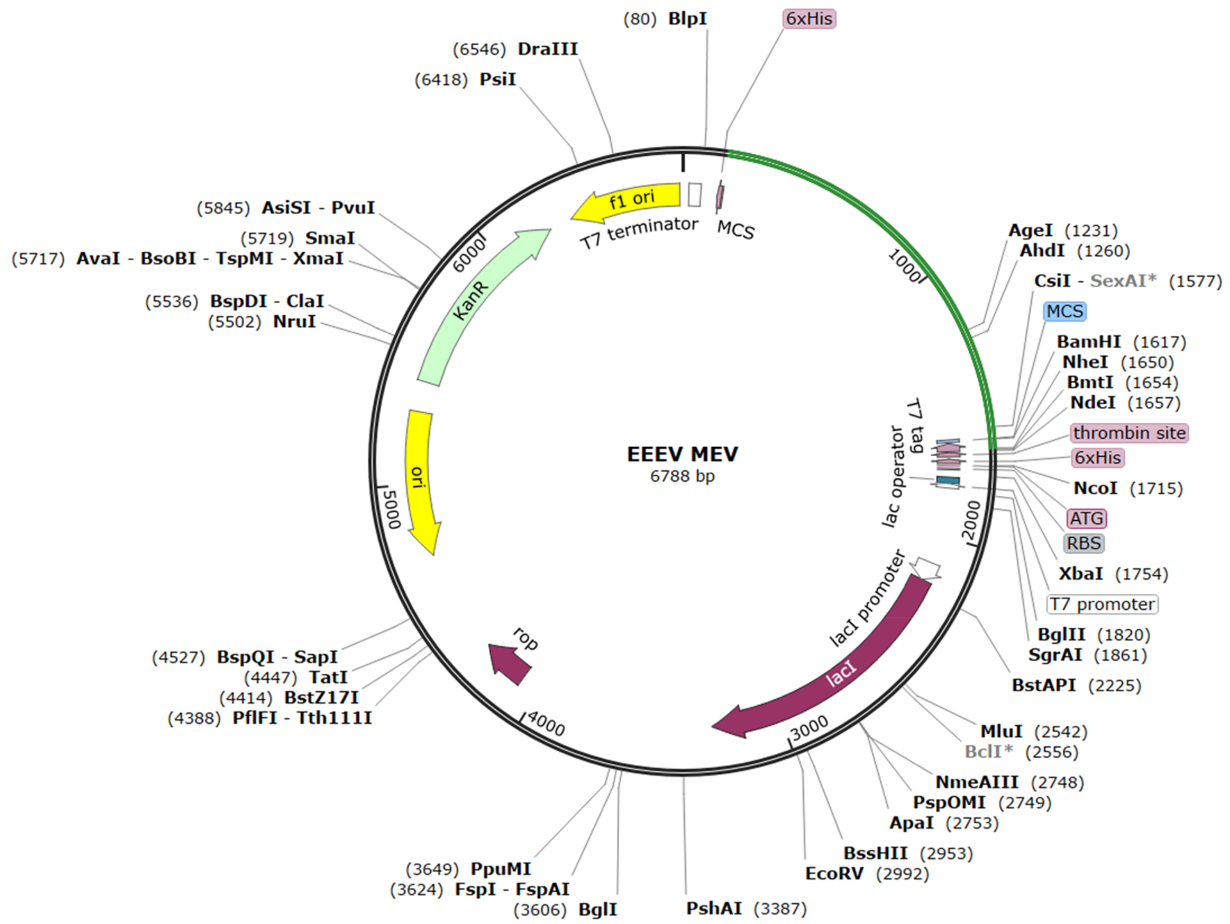

Figure 10. EEEV vaccine candidate in silico cloning.

candidate for EEEV was determined using VaxiJen version 2.0 tool.

Computational Immunosimulation of the EEEV-MEV. To examine the immune response generated by immunizing with the EEEV vaccine, an in silico immune simulation was performed by the C-IMMSIM tool.[49] The software's default settings were utilized except for the time step. It is generally recommended to have a minimum duration of 4 weeks between two consecutive vaccine doses, although in some cases, a longer interval may also be considered.[50,51] Therefore, the EEEV vaccine's immune response profile was assessed by administering three doses at four-week intervals. The simulation employed time steps of 1, 84 (≈4 weeks), and 168 (≈8 weeks).

Molecular Modeling, Molecular Docking, and Molecular Dynamics Simulation Studies. The 3D structure prediction of the EEEV and human TLR5 proteins was conducted using a deep learning approach of AlphaFold2 via ColabFold (https://colab.research.google.com/github/sokrypton/ColabFold/blob/main/AlphaFold2.ipynb).[24,52] The accuracy of the predicted tertiary structures was validated using the QMEANS4 score[53] and ProCheck Web server.[54] To dock EEEV-MEV with TLR5, the HADDOCK server[55] was employed, utilizing default settings. Subsequently, to assess the stability of the docked complex, molecular dynamics (MD) simulations were performed using the GROMACS 2022 simulation program.[56] The TLR5 protein complexed with EEEV was placed in a cubic box and solvated with TIP3P water molecules, creating a solvent layer that was at least 10 Å thick. The Amber ff99SB-ILDN force field was used to model the parameters of the proteins.[57] Charge neutralization was achieved by adding Cl^- ions. The simulation box contained 251,920 water molecules, resulting in a total of 772,647 atoms in the system. System minimization was performed using the steepest descent method, applying a position restraint of 1000 kJ/mol nm^2 on the heavy atoms of the protein. The equilibration process was carried out in a phased manner. Initially, a 1 ns NVT simulation was performed, followed by a 1 ns NPT simulation with restraints on the heavy atoms of the protein. Subsequently, a 10 ns equilibration without restraints on atoms was conducted by using the NPT ensemble. The structure obtained after 10 ns of MD simulation was utilized as the starting structure for further equilibration and production simulations. Production simulations were run for 100 ns using the NPT ensemble, maintaining a temperature of 300 K with velocity rescaling and a coupling time of 0.1 ps. The pressure was maintained at 1 atm using a Parrinello–Rahman barostat with a coupling time of 2 ps.[58] The equations of motion were integrated using the leapfrog algorithm with a time step of 2.0 fs. The particle mesh Ewald (PME) method was employed for evaluating electrostatic interactions.[59] A cutoff value of 1 nm was utilized for van der Waals and Coulombic interactions. Periodic boundary conditions (PBCs) were applied in all directions to mimic the bulk behavior. The LINCS algorithm was employed to constrain bonds involving hydrogen atoms.[60] The trajectory was saved every 10 ps, and subsequent trajectory processing and analysis were performed by using GROMACS tools. Visualization and generation of molecular

https://doi.org/10.1021/acsomega.3c07322
ACS Omega 2024, 9, 1092−1105

graphics images were accomplished using PyMOL and VMD software.[61]

Codon Adaptation and Computational Cloning of the Designed EEEV Vaccine. The JCat server was employed to optimize the codons of the vaccine construct gene for expression in the *E. coli* 06 strain 536.[62] This optimization process aimed to ensure successful cloning and presentation of the vaccine construct in the expression vectors. As described by Hasan et al., codon optimization also involved the removal of cleavage sites for various restriction enzymes, prokaryotic ribosomal binding sites, and rho-independent transcription terminators.[63] To facilitate the in silico cloning process, the SnapGene restriction cloning module developed by Insightful Science was utilized.

■ ASSOCIATED CONTENT

Supporting Information

The Supporting Information is available free of charge at https://pubs.acs.org/doi/10.1021/acsomega.3c07322.

Predicted structural assessments of TLR5, dynamic behavior, and interaction characteristics of TLR5 and EEEV vaccine constructs, along with immune properties of epitopes and codon usage details (PDF)

Chosen HLA alleles for predicting T-helper cell epitopes and T-cytotoxic cell epitopes and B-cell epitopes data (ZIP)

■ AUTHOR INFORMATION

Corresponding Author

Heebal Kim − *Department of Agricultural Biotechnology and Research Institute of Agriculture and Life Sciences and Interdisciplinary Program in Bioinformatics, Seoul National University, Seoul 08826, Republic of Korea; eGnome, Inc., Seoul 05836, Republic of Korea*; Phone: +82 2 880 4802; Email: heebal@snu.ac.kr; Fax: +82 2 883 8812

Author

Truc Ly Nguyen − *Department of Agricultural Biotechnology and Research Institute of Agriculture and Life Sciences, Seoul National University, Seoul 08826, Republic of Korea*; orcid.org/0000-0001-8843-1072

Complete contact information is available at: https://pubs.acs.org/10.1021/acsomega.3c07322

Author Contributions

T.L.N. and H.K.: Conceptualization, Methodology, Validation, Formal analysis, Investigation, Visualization, Writing−original draft, Writing−review and editing; H.K.: Supervision. Both authors read and approved the submitted version.

Notes

The authors declare no competing financial interest.

■ ACKNOWLEDGMENTS

The authors are thankful to the laboratory of Bioinformatics and Population genetics, Seoul National University, for providing the computing infrastructure to implement and execute the research work. This work was supported by the BK21 FOUR Program of the Department of Agricultural Biotechnology, Seoul National University, Seoul, Republic of Korea.

■ REFERENCES

(1) Armstrong, P. M.; Andreadis, T. G. Ecology and Epidemiology of Eastern Equine Encephalitis Virus in the Northeastern United States: An Historical Perspective. *Journal of medical entomology* **2022**, *59* (1), 1−13.

(2) Corrin, T.; Ackford, R.; Mascarenhas, M.; Greig, J.; Waddell, L. A. Eastern Equine Encephalitis Virus: A Scoping Review of the Global Evidence. *Vector Borne Zoonotic Dis* **2021**, *21* (5), 305−320.

(3) Ciota, A. T. Eastern Equine Encephalitis Virus Taxonomy, Genomics, and Evolution. *Journal of Medical Entomology* **2022**, *59* (1), 14−19.

(4) Carrera, J.-P.; Forrester, N.; Wang, E.; Vittor, A. Y.; Haddow, A. D.; López-Vergès, S.; Abadía, I.; Castaño, E.; Sosa, N.; Báez, C.; et al. Eastern equine encephalitis in Latin America. *N Engl J. Med.* **2013**, *369* (8), 732−744.

(5) Bonilla-Aldana, D. K.; Bonilla Carvajal, C. D.; Moreno-Ramos, E.; Barboza, J. J.; Rodriguez-Morales, A. J. Mapping Eastern (EEE) and Venezuelan Equine Encephalitides (VEE) among Equines Using Geographical Information Systems, Colombia, 2008−2019. *Viruses* **2023**, *15* (3), 707.

(6) Sah, R.; Siddiq, A.; Al-Ahdal, T.; Maulud, S. Q.; Mohanty, A.; Padhi, B. K.; El-Shall, N. A.; Chandran, D.; Emran, T. B.; Hussein, N. R. The emerging scenario for the Eastern equine encephalitis virus and mitigation strategies to counteract this deadly mosquito-borne zoonotic virus, the cause of the most severe arboviral encephalitis in humans—an update. *Frontiers in Tropical Diseases* **2023**, *3*, 1.

(7) Ladzinski, A. T.; Tai, A.; Rumschlag, M. T.; Smith, C. S.; Mehta, A.; Boapimp, P.; Edewaard, E. J.; Douce, R. W.; Morgan, L. F.; Wang, M. S.; et al. Clinical Characteristics of the 2019 Eastern Equine Encephalitis Outbreak in Michigan. *Open Forum Infect Dis* **2023**, *10* (5), ofad206−ofad206.

(8) Morens, D. M.; Folkers, G. K.; Fauci, A. S. Eastern Equine Encephalitis Virus — Another Emergent Arbovirus in the United States. *New England Journal of Medicine* **2019**, *381* (21), 1989−1992.

(9) Reddy, A. J.; Woods, C. W.; Welty-Wolf, K. E. Eastern equine encephalitis leading to multi-organ failure and sepsis. *Journal of Clinical Virology* **2008**, *42* (4), 418−421.

(10) Powers, A. M. Resurgence of Interest in Eastern Equine Encephalitis Virus Vaccine Development. *Journal of Medical Entomology* **2022**, *59* (1), 20−26.

(11) Lindsey, N. P.; Staples, J. E.; Fischer, M. Eastern Equine Encephalitis Virus in the United States, 2003−2016. *Am. J. Trop Med. Hyg* **2018**, *98* (5), 1472−1477.

(12) Fothergill, L. D.; Dingle, J. H.; Farber, S.; Connerley, M. L. Human Encephalitis Caused by the Virus of the Eastern Variety of Equine Encephalomyelitis. *New England Journal of Medicine* **1938**, *219* (12), 411−411.

(13) Lindsey, N. P.; Martin, S. W.; Staples, J. E.; Fischer, M. Notes from the Field: Multistate Outbreak of Eastern Equine Encephalitis Virus - United States, 2019. *MMWR Morb Mortal Wkly Rep* **2020**, *69* (2), 50−51.

(14) Hill, V.; Koch, R. T.; Bialosuknia, S. M.; Ngo, K.; Zink, S. D.; Koetzner, C. A.; Maffei, J. G.; Dupuis, A. P.; Backenson, P. B.; Oliver, J. Dynamics of Eastern equine encephalitis virus during the 2019 outbreak in the Northeast United States. *Current Biology* **2023**, *33*, 2515.

(15) Pierson, B. C.; Cardile, A. P.; Okwesili, A. C.; Downs, I. L.; Reisler, R. B.; Boudreau, E. F.; Kortepeter, M. G.; Koca, C. D.; Ranadive, M. V.; Petitt, P. L.; et al. Safety and immunogenicity of an inactivated eastern equine encephalitis virus vaccine. *Vaccine* **2021**, *39* (20), 2780−2790.

(16) Coates, E. E.; Edupuganti, S.; Chen, G. L.; Happe, M.; Strom, L.; Widge, A.; Florez, M. B.; Cox, J. H.; Gordon, I.; Plummer, S.; et al. Safety and immunogenicity of a trivalent virus-like particle vaccine against western, eastern, and Venezuelan equine encephalitis viruses: a phase 1, open-label, dose-escalation, randomised clinical trial. *Lancet Infect. Dis.* **2022**, *22* (8), 1210−1220.

https://doi.org/10.1021/acsomega.3c07322
ACS Omega 2024, 9, 1092−1105

(17) Zhang, L. Multi-epitope vaccines: a promising strategy against tumors and viral infections. *Cell Mol. Immunol* **2018**, *15* (2), 182−184.

(18) Jacchieri, S. G.; Torquato, R.; Brentani, R. R. Structural Study of Binding of Flagellin by Toll-Like Receptor 5. *J. Bacteriol.* **2003**, *185* (14), 4243−4247.

(19) Kaushik, V.; Jain, P.; Akhtar, N.; Joshi, A.; Gupta, L. R.; Grewal, R. K.; Oliva, R.; Shaikh, A. R.; Cavallo, L.; Chawla, M. Immunoinformatics-Aided Design and In Vivo Validation of a Peptide-Based Multiepitope Vaccine Targeting Canine Circovirus. *ACS Pharmacology & Translational Science* **2022**, *5* (8), 679−691.

(20) Kaushik, V.; G, S. K.; Gupta, L. R.; Kalra, U.; Shaikh, A. R.; Cavallo, L.; Chawla, M. Immunoinformatics Aided Design and In-Vivo Validation of a Cross-Reactive Peptide Based Multi-Epitope Vaccine Targeting Multiple Serotypes of Dengue Virus. *Frontiers in immunology* **2022**, *13*, 865180−865180.

(21) Vangone, A.; Spinelli, R.; Scarano, V.; Cavallo, L.; Oliva, R. COCOMAPS: a web application to analyze and visualize contacts at the interface of biomolecular complexes. *Bioinformatics* **2011**, *27* (20), 2915−2916.

(22) Laskowski, R. A.; Jabłońska, J.; Pravda, L.; Vařeková, R. S.; Thornton, J. M. PDBsum: Structural summaries of PDB entries. *Protein Sci.* **2018**, *27* (1), 129−134.

(23) Tan, Y.; Lam, T. T.-Y.; Heberlein-Larson, L. A.; Smole, S. C.; Auguste, A. J.; Hennigan, S.; Halpin, R. A.; Fedorova, N.; Puri, V.; Stockwell, T. B.; et al. Large-Scale Complete-Genome Sequencing and Phylodynamic Analysis of Eastern Equine Encephalitis Virus Reveals Source-Sink Transmission Dynamics in the United States. *J. Virol* **2018**, *92* (12), e00074−00018.

(24) Jumper, J.; Evans, R.; Pritzel, A.; Green, T.; Figurnov, M.; Ronneberger, O.; Tunyasuvunakool, K.; Bates, R.; Žídek, A.; Potapenko, A.; et al. Highly accurate protein structure prediction with AlphaFold. *Nature* **2021**, *596* (7873), 583−589.

(25) Hasan, S. S.; Dey, D.; Singh, S.; Martin, M. The Structural Biology of Eastern Equine Encephalitis Virus, an Emerging Viral Threat. *Pathogens (Basel, Switzerland)* **2021**, *10* (8), 973.

(26) Aguilar, P. V.; Adams, A. P.; Wang, E.; Kang, W.; Carrara, A.-S.; Anishchenko, M.; Frolov, I.; Weaver, S. C. Structural and non-structural protein genome regions of eastern equine encephalitis virus are determinants of interferon sensitivity and murine virulence. *J. Virol* **2008**, *82* (10), 4920−4930.

(27) Dupuy, L. C.; Richards, M. J.; Livingston, B. D.; Hannaman, D.; Schmaljohn, C. S. A Multiagent Alphavirus DNA Vaccine Delivered by Intramuscular Electroporation Elicits Robust and Durable Virus-Specific Immune Responses in Mice and Rabbits and Completely Protects Mice against Lethal Venezuelan, Western, and Eastern Equine Encephalitis Virus Aerosol Challenges. *J. Immunol Res.* **2018**, *2018*, 8521060.

(28) Hu, W.-G.; Steigerwald, R.; Kalla, M.; Volkmann, A.; Noll, D.; Nagata, L. P. Protective efficacy of monovalent and trivalent recombinant MVA-based vaccines against three encephalitic alphaviruses. *Vaccine* **2018**, *36* (34), 5194−5203.

(29) Phillips, A. T.; Schountz, T.; Toth, A. M.; Rico, A. B.; Jarvis, D. L.; Powers, A. M.; Olson, K. E. Liposome-antigen-nucleic acid complexes protect mice from lethal challenge with western and eastern equine encephalitis viruses. *J. Virol* **2014**, *88* (3), 1771−1780.

(30) Pandya, J.; Gorchakov, R.; Wang, E.; Leal, G.; Weaver, S. C. A vaccine candidate for eastern equine encephalitis virus based on IRES-mediated attenuation. *Vaccine* **2012**, *30* (7), 1276−1282.

(31) Ko, S.-Y.; Akahata, W.; Yang, E. S.; Kong, W.-P.; Burke, C. W.; Honnold, S. P.; Nichols, D. K.; Huang, Y.-J. S.; Schieber, G. L.; Carlton, K. A virus-like particle vaccine prevents equine encephalitis virus infection in nonhuman primates. *Science Translational Medicine* **2019**, *11* (492), 1.

(32) Coates, E. E.; Edupuganti, S.; Chen, G. L.; Happe, M.; Strom, L.; Widge, A.; Florez, M. B.; Cox, J. H.; Gordon, I.; Plummer, S.; et al. Safety and immunogenicity of a trivalent virus-like particle vaccine against western, eastern, and Venezuelan equine encephalitis viruses: a phase 1, open-label, dose-escalation, randomised clinical trial. *Lancet Infect Dis* **2022**, *22* (8), 1210−1220.

(33) The UniProt Consortium. UniProt: the Universal Protein Knowledgebase in 2023. *Nucleic Acids Res.* **2023**, *51* (D1), D523−D531.

(34) Jensen, K. K.; Andreatta, M.; Marcatili, P.; Buus, S.; Greenbaum, J. A.; Yan, Z.; Sette, A.; Peters, B.; Nielsen, M. Improved methods for predicting peptide binding affinity to MHC class II molecules. *Immunology* **2018**, *154* (3), 394−406.

(35) Jurtz, V.; Paul, S.; Andreatta, M.; Marcatili, P.; Peters, B.; Nielsen, M. NetMHCpan-4.0: Improved Peptide-MHC Class I Interaction Predictions Integrating Eluted Ligand and Peptide Binding Affinity Data. *J. Immunol* **2017**, *199* (9), 3360−3368.

(36) Larsen, J. E. P.; Lund, O.; Nielsen, M. Improved method for predicting linear B-cell epitopes. *Immunome Res.* **2006**, *2*, 2−2.

(37) Doytchinova, I. A.; Flower, D. R. VaxiJen: a server for prediction of protective antigens, tumour antigens and subunit vaccines. *BMC bioinformatics* **2007**, *8*, 4−4.

(38) Gupta, S.; Kapoor, P.; Chaudhary, K.; Gautam, A.; Kumar, R.; Open Source Drug Discovery Consortium; Raghava, G. P. S. In silico approach for predicting toxicity of peptides and proteins. *PloS one* **2013**, *8* (9), e73957−e73957.

(39) Dimitrov, I.; Naneva, L.; Doytchinova, I.; Bangov, I. AllergenFP: allergenicity prediction by descriptor fingerprints. *Bioinformatics* **2014**, *30* (6), 846−851.

(40) Dhanda, S. K.; Vir, P.; Raghava, G. P. S. Designing of interferon-gamma inducing MHC class-II binders. *Biol. Direct* **2013**, *8*, 30−30.

(41) Dhanda, S. K.; Gupta, S.; Vir, P.; Raghava, G. P. S. Prediction of IL4 inducing peptides. *Clin Dev Immunol* **2013**, *2013*, 263952.

(42) Kim, Y.; Ponomarenko, J.; Zhu, Z.; Tamang, D.; Wang, P.; Greenbaum, J.; Lundegaard, C.; Sette, A.; Lund, O.; Bourne, P. E.; et al. Immune epitope database analysis resource. *Nucleic Acids Res.* **2012**, *40* (W1), W525−W530.

(43) Mugunthan, S. P.; Harish, M. C. Multi-epitope-Based Vaccine Designed by Targeting Cytoadherence Proteins of *Mycoplasma gallisepticum*. *ACS Omega* **2021**, *6* (21), 13742−13755.

(44) Sami, S. A.; Marma, K. K. S.; Mahmud, S.; Khan, M. A. N.; Albogami, S.; El-Shehawi, A. M.; Rakib, A.; Chakraborty, A.; Mohiuddin, M.; Dhama, K.; et al. Designing of a Multi-epitope Vaccine against the Structural Proteins of Marburg Virus Exploiting the Immunoinformatics Approach. *ACS Omega* **2021**, *6* (47), 32043−32071.

(45) Nguyen, T. L.; Samuel Leon Magdaleno, J.; Rajjak Shaikh, A.; Choowongkomon, K.; Li, V.; Lee, Y.; Kim, H. Designing a multi-epitope candidate vaccine by employing immunoinformatics approaches to control African swine fever spread. *J. Biomol. Struct. Dyn.* **2022**, 1−16.

(46) Akhtar, N.; Singh, A.; Upadhyay, A. K.; Mannan, M. A.-U. Design of a multi-epitope vaccine against the pathogenic fungi Candida tropicalis using an in silico approach. *J. Genet Eng. Biotechnol* **2022**, *20* (1), 140−140.

(47) Akhtar, N.; Magdaleno, J. S. L.; Ranjan, S.; Wani, A. K.; Grewal, R. K.; Oliva, R.; Shaikh, A. R.; Cavallo, L.; Chawla, M. Secreted Aspartyl Proteinases Targeted Multi-Epitope Vaccine Design for Candida dubliniensis Using Immunoinformatics. *Vaccines* **2023**, *11* (2), 364.

(48) Akhtar, N.; Kaushik, V.; Grewal, R. K.; Wani, A. K.; Suwattanasophon, C.; Choowongkomon, K.; Oliva, R.; Shaikh, A. R.; Cavallo, L.; Chawla, M. Immunoinformatics-Aided Design of a Peptide Based Multiepitope Vaccine Targeting Glycoproteins and Membrane Proteins against Monkeypox Virus. *Viruses* **2022**, *14* (11), 2374.

(49) Rapin, N.; Lund, O.; Castiglione, F. Immune system simulation online. *Bioinformatics* **2011**, *27* (14), 2013−2014.

(50) Robinson, C. L.; Romero, J. R.; Kempe, A.; Pellegrini, C. Advisory Committee on Immunization Practices Child/Adolescent Immunization Work, G. Advisory Committee on Immunization Practices Recommended Immunization Schedule for Children and

Adolescents Aged 18 Years or Younger - United States, 2017. *MMWR Morb Mortal Wkly Rep* **2017**, *66* (5), 134−135.

(51) Castiglione, F.; Mantile, F.; De Berardinis, P.; Prisco, A. How the interval between prime and boost injection affects the immune response in a computational model of the immune system. *Comput. Math Methods Med.* **2012**, *2012*, 842329.

(52) David, A.; Islam, S.; Tankhilevich, E.; Sternberg, M. J. E. The AlphaFold Database of Protein Structures: A Biologist's Guide. *Journal of molecular biology* **2022**, *434* (2), 167336−167336.

(53) Benkert, P.; Biasini, M.; Schwede, T. Toward the estimation of the absolute quality of individual protein structure models. *Bioinformatics* **2011**, *27* (3), 343−350.

(54) Laskowski, R.; Rullmann, J. A.; Macarthur, M.; Kaptein, R.; Thornton, J. AQUA and PROCHECK-NMR: Programs for checking the quality of protein structures solved by NMR. *Journal of Biomolecular NMR* **1996**, *8* (4), 477−486.

(55) van Zundert, G. C. P.; Rodrigues, J. P. G. L. M.; Trellet, M.; Schmitz, C.; Kastritis, P. L.; Karaca, E.; Melquiond, A. S. J.; van Dijk, M.; de Vries, S. J.; Bonvin, A. M. J. J. The HADDOCK2.2 Web Server: User-Friendly Integrative Modeling of Biomolecular Complexes. *J. Mol. Biol.* **2016**, *428* (4), 720−725.

(56) Abraham, M. J.; Murtola, T.; Schulz, R.; Páll, S.; Smith, J. C.; Hess, B.; Lindahl, E. GROMACS: High performance molecular simulations through multi-level parallelism from laptops to supercomputers. *SoftwareX* **2015**, *1−2*, 19−25.

(57) Lindorff-Larsen, K.; Piana, S.; Palmo, K.; Maragakis, P.; Klepeis, J. L.; Dror, R. O.; Shaw, D. E. Improved side-chain torsion potentials for the Amber ff99SB protein force field. *Proteins* **2010**, *78* (8), 1950−1958.

(58) Parrinello, M.; Rahman, A. Polymorphic transitions in single crystals: A new molecular dynamics method. *J. Appl. Phys.* **1981**, *52* (12), 7182−7190.

(59) Darden, T.; York, D.; Pedersen, L. Particle mesh Ewald: An $N\cdot\log(N)$ method for Ewald sums in large systems. *J. Chem. Phys.* **1993**, *98* (12), 10089−10092.

(60) Hess, B.; Bekker, H.; Berendsen, H. J. C.; Fraaije, J. G. E. M. LINCS: A linear constraint solver for molecular simulations. *J. Comput. Chem.* **1997**, *18* (12), 1463−1472.

(61) Humphrey, W.; Dalke, A.; Schulten, K. VMD: Visual molecular dynamics. *J. Mol. Graphics* **1996**, *14* (1), 33−38.

(62) Grote, A.; Hiller, K.; Scheer, M.; Münch, R.; Nörtemann, B.; Hempel, D. C.; Jahn, D. JCat: a novel tool to adapt codon usage of a target gene to its potential expression host. *Nucleic acids research* **2005**, *33*, W526−W531.

(63) Hasan, M.; Islam, M. S.; Chakraborty, S.; Mustafa, A. H.; Azim, K. F.; Joy, Z. F.; Hossain, M. N.; Foysal, S. H.; Hasan, M. N. Contriving a chimeric polyvalent vaccine to prevent infections caused by Herpes Simplex Virus (Type-1 and Type-2): an exploratory immunoinformatic approach. *Journal of Biomolecular Structure and Dynamics* **2020**, *38*, 2898−2915.